Eureka Open Access Journals
Open Access | Peer Reviewed | International Journals | Multidisciplinary Areas

Eureka Journal of Geoscience, Materials & Resource Engineering (EJGMRE)

ISSN 2760-4985 (Online) Volume 02, Issue 05, May 2026

https://eurekaoa.com/index.php/9

RARE-EARTH ADDITIONS AND AGING EFFECTS ON AZ31 MAGNESIUM ALLOY: MICROSTRUCTURE, CORROSION, AND WEAR

Sarah Khazaal Jabbar Madhi1
Department of Metallurgical and Materials Engineering,
Al-Turath University, Baghdad, Iraq
Corresponding author: sarah.khazaal@uoturath.edu.iq
ORCID: S. K. J. Madhi: https://orcid.org/0009-0003-7501-9814

Abstract

Magnesium alloys are promising biodegradable orthopedic implant candidates due to their bone-compatible elastic modulus and density, but suffer from rapid corrosion in physiological media. This study investigates the combined effect of minor rare-earth (Nd, La) additions and isothermal aging at 180 °C on the microstructure, mechanical properties, wear, and electrochemical corrosion behavior of AZ31 magnesium alloy in 3.5 wt.% NaCl and simulated body fluid (SBF). Four compositions were produced by low-pressure permanent-mold casting and aged from 10 min to 3 h. Rare-earth additions promoted fine $Al_{11}La_3$, Al_2La, and Al-Nd intermetallics along grain boundaries. The optimized AZ31-0.5Nd-0.5La alloy aged 3 h achieved a 39% increase in Vickers hardness (56→78 HV), compressive yield strength of 148 MPa, and a corrosion current density of 1.14 µA/cm² in NaCl (87% reduction vs. as-cast AZ31). The highest polarization resistance (≈24.6 kΩ·cm²) was recorded in SBF. Bio-tribocorrosion synergy elevated wear rates in biological media despite reduced friction coefficients. These results position AZ31-0.5Nd-0.5La aged 3 h as a promising candidate for biodegradable orthopedic applications, pending in vitro and in vivo biological validation.

Eureka Open Access Journals
Open Access | Peer Reviewed | International Journals | Multidisciplinary Areas

Eureka Journal of Geoscience, Materials & Resource Engineering (EJGMRE)

ISSN 2760-4985 (Online) Volume 02, Issue 05, May 2026

https://eurekaoa.com/index.php/9

Keywords: AZ31 magnesium alloy; rare-earth elements; aging heat treatment; electrochemical corrosion; biodegradable implant.

1. Introduction

The design of metallic biomaterials capable of providing adequate mechanical support during bone healing while subsequently dissolving safely within the body remains one of the most demanding objectives in contemporary biomedical engineering [1,2]. Permanent metallic implants based on titanium, cobalt-chromium, and 316L stainless steel offer excellent durability but are associated with several recognized drawbacks, including stress shielding caused by the large mismatch in elastic modulus relative to bone, the requirement for a second surgical intervention to remove the implant after healing, and the gradual release of potentially toxic ions into surrounding tissues [3,4]. Biodegradable metallic systems based on magnesium, zinc, and iron have therefore emerged as a fundamentally different family of orthopedic materials [5–7].

Among biodegradable metals, magnesium alloys exhibit a uniquely favorable combination of physical and biological attributes. Their density (~1.74 g/cm^3) is approximately four times lower than that of stainless steel, and their elastic modulus (41–45 GPa) is markedly closer to that of human cortical bone (10–25 GPa) than any conventional implant alloy [8,9]. Magnesium is, in addition, an essential nutrient involved in numerous enzymatic and structural processes, and its corrosion products can in principle be metabolized and eliminated through natural physiological pathways [10]. The high chemical reactivity of magnesium in chloride-containing physiological fluids, however, leads to rapid corrosion accompanied by hydrogen evolution, which can compromise mechanical integrity before bone healing is complete [11,12].

The AZ31 alloy has been widely investigated as a candidate substrate because Al and Zn improve castability and provide moderate solid-solution strengthening, while Mn sequesters detrimental iron impurities that would otherwise act as

Eureka Open Access Journals
Open Access | Peer Reviewed | International Journals | Multidisciplinary Areas
OPEN ACCESS JOURNALS

Eureka Journal of Geoscience, Materials & Resource Engineering (EJGMRE)

ISSN 2760-4985 (Online) Volume 02, Issue 05, May 2026

https://eurekaoa.com/index.php/9

cathodic sites and accelerate galvanic corrosion [14,15]. Among the rare-earth (RE) elements proposed as alloying additions, Nd and La are particularly attractive owing to their low cytotoxicity, grain-refining capability, and tendency to form thermally stable intermetallic phases with aluminum [16–18]. Aging heat treatment activates the precipitation of secondary phases that can act as barriers against the lateral propagation of corrosion, but this effect must be balanced against grain coarsening and the possible galvanic activity of coarse second-phase networks [20,21].

Lwin et al. [31] recently confirmed that single and combined additions of rare-earth elements (Nd and Dy) to AZ31 improve corrosion resistance through the formation of Al-RE phases, while Abdelfattah et al. [32] demonstrated that microstructural refinement strongly modulates the corrosion–degradation balance of biomedical AZ31. Despite these advances, the combined influence of Nd and La additions in the specific compositional window of 0.1–0.5 wt.% La together with 0.5 wt.% Nd, and the time-resolved evolution of properties during aging at 180 °C, has not been comprehensively reported in the open literature. The present study addresses this gap.

The specific objectives of this work are: (i) to fabricate four AZ31-based compositions containing 0.5 wt.% Nd and 0.1–0.5 wt.% La by low-pressure permanent-mold casting; (ii) to apply isothermal aging at 180 °C for soaking times ranging from 10 min to 3 h; (iii) to characterize the resulting microstructure, mechanical properties, and density; (iv) to evaluate dry-sliding and bio-tribological behavior in Hank's balanced salt solution; (v) to determine the corrosion response by mass-loss immersion, potentiodynamic polarization, and EIS in 3.5 wt.% NaCl and Kokubo-type SBF; and (vi) to propose a mechanistic interpretation of the observed improvements that may guide future Mg-RE alloy design for biodegradable orthopedic applications.

Eureka Open Access Journals
Open Access | Peer Reviewed | International Journals | Multidisciplinary Areas

Eureka Journal of Geoscience, Materials & Resource Engineering (EJGMRE)

ISSN 2760-4985 (Online) Volume 02, Issue 05, May 2026

https://eurekaoa.com/index.php/9

1.1. Corrosion Mechanisms in Physiological Media

The overall corrosion reaction $Mg + 2H_2O \rightarrow Mg(OH)_2 + H_2$ produces a magnesium hydroxide film. Although $Mg(OH)_2$ is partially passive at high pH, it is rapidly converted to soluble $MgCl_2$ in the presence of chloride ions, sustaining a relatively high corrosion rate [28,29]. Recent reviews [33] have emphasized that, in biomedical contexts, Mg degradation is further complicated by the presence of carbonates, phosphates, organic species, and dynamic flow conditions. Dominant degradation morphologies include localized pitting, intergranular attack, micro-galvanic coupling between the α-Mg matrix and second-phase particles, and fretting/tribocorrosion phenomena under physiological loading. All of these mechanisms are sensitive to alloy composition, microstructure, and electrolyte chemistry [28,33].

1.2. Role of Rare-Earth Elements

Lanthanum and neodymium restrict grain growth during solidification, combine with aluminum to form thermally stable intermetallic compounds, and—in the case of La—act as scavengers for harmful Fe and Si impurities that would otherwise generate strong cathodic sites [16]. Nd contributes additional solid-solution strengthening and promotes the precipitation of fine Al-Nd phases. The simultaneous addition of Nd and La in optimized proportions has been shown to deliver synergistic improvements in mechanical and corrosion behavior, provided that the aging schedule is correctly designed [16–18,31]. A recent comprehensive review on Mg-RE biomaterials [34] further emphasizes that Nd is particularly effective in suppressing hydrogen embrittlement, while La contributes to passive-layer stability—observations that directly motivate the present study.

1. Literature Review

A growing body of literature confirms that rare-earth (RE) alloying and thermomechanical processing are effective strategies for improving the corrosion

Eureka Open Access Journals
Open Access | Peer Reviewed | International Journals | Multidisciplinary Areas
OPEN ACCESS JOURNALS

Eureka Journal of Geoscience, Materials & Resource Engineering (EJGMRE)

ISSN 2760-4985 (Online) Volume 02, Issue 05, May 2026

https://eurekaoa.com/index.php/9

resistance and mechanical performance of AZ-series magnesium alloys. Staiger et al. [5] established the foundational case for Mg-based biodegradable implants, highlighting their density and modulus compatibility with cortical bone. Hort et al. [16] demonstrated that Mg-RE alloys exhibit superior corrosion resistance through the formation of stable Al-RE intermetallic networks, while Tekumalla et al. [17] reviewed the breadth of mechanical property improvements achievable by RE additions. Lwin et al. [31] recently confirmed that single and combined additions of Nd and Dy to AZ31 promote Al-RE phase formation that reduces corrosion rates in NaCl solution. Abdelfattah et al. [32] showed that microstructural refinement of AZ31 via severe plastic deformation significantly modulates its degradation kinetics in SBF. Yavuzyegit et al. [33] evaluated AZ31 corrosion performance in multiple physiological solutions and underscored the sensitivity of corrosion mechanisms to electrolyte chemistry. Senthilkumar et al. [34] provided a comprehensive review of RE-based Mg alloys as biomaterials, emphasizing that Nd suppresses hydrogen embrittlement and La stabilizes passive oxide films. Despite these advances, the combined influence of Nd and La additions in the 0.1–0.5 wt.% La compositional window, together with time-resolved aging at 180 °C, has not been comprehensively reported. Table LR1 summarizes the key literature works most relevant to the present study.

Eureka Open Access Journals
Open Access | Peer Reviewed | International Journals | Multidisciplinary Areas

Eureka Journal of Geoscience, Materials & Resource Engineering (EJGMRE)

ISSN 2760-4985 (Online) Volume 02, Issue 05, May 2026

https://eurekaoa.com/index.php/9

Table LR1. Summary of key literature works related to the present study.

Reference	Year	Material / System	Key Finding	Relevance to Present Work
Staiger et al. [5]	2006	Mg alloys as orthopedic biomaterials	Density and modulus compatible with cortical bone	Basis for biomedical candidacy of AZ31
Hort et al. [16]	2010	Mg-RE alloys (Gd, Y, Nd, La)	Al-RE phases reduce corrosion; principles of Mg-RE alloy design	Direct mechanistic basis for Nd + La selection
Lwin et al. [31]	2024	AZ31 + Nd + Dy additions	Combined RE improves corrosion via Al-RE phase continuity	Most relevant prior work; La replaces Dy here
Abdelfattah et al. [32]	2025	MCSTE-processed AZ31 in SBF	Microstructural refinement modulates degradation in SBF	Benchmark for i_corr comparison in SBF
Senthilkumar et al. [34]	2024	Review: Mg-RE biomaterial alloys	Nd suppresses H embrittlement; La stabilizes passive film	Justifies Nd + La combination chosen here

2. Materials and Methods

2.1. Alloy Fabrication

Commercially pure Mg, Al, Zn, and Mg-Nd / Mg-La master alloys were melted and cast by low-pressure permanent-mold casting under argon protection at 775 °C. The melt was injected into a stainless-steel mold preheated to 350 °C under an applied pressure of 2–3 atm. Final compositions were verified by spark optical emission spectroscopy (OES) and are reported in Table 1. Slight variations in Al and Zn between compositions are inherent to the master-alloy mixing route adopted; their potential contribution to the corrosion response is explicitly considered alongside the dominant effect of Nd and La additions in Section 3.6.

Eureka Open Access Journals
Open Access | Peer Reviewed | International Journals | Multidisciplinary Areas

Eureka Journal of Geoscience, Materials & Resource Engineering (EJGMRE)

ISSN 2760-4985 (Online) Volume 02, Issue 05, May 2026

https://eurekaoa.com/index.php/9

Table 1. Chemical composition (wt.%) of the four AZ31-based alloys, measured by spark OES (mean of three readings).

Alloy	Al	Mn	Zn	Nd	La	Mg
AZ31	3.62	0.11	1.18	—	—	Bal.
AZ31-0.5Nd-0.1La	3.01	0.27	0.95	0.48	0.11	Bal.
AZ31-0.5Nd-0.2La	2.92	0.15	0.91	0.49	0.23	Bal.
AZ31-0.5Nd-0.5La	2.88	0.25	0.87	0.45	0.54	Bal.

Note: Compositional variations in Al and Zn between alloys are an inherent consequence of the master-alloy dilution route and do not represent targeted modifications; their secondary contribution to the observed corrosion response is discussed quantitatively in Section 3.6.

2.2. Heat Treatment

Specimens were aged in an electric muffle furnace at 180 ± 2 °C for soaking times of 10, 20, 30, and 40 min and 1, 2, and 3 h, followed by slow cooling within the furnace. After aging, surfaces were ground successively up to 2000-grit SiC paper, polished with 1 μm diamond suspension, and ultrasonically cleaned in absolute ethanol prior to all subsequent characterization.

2.3. Microstructural Characterization

Etched surfaces (acetic-picral solution) were examined by optical microscopy and by a Carl Zeiss EVO scanning electron microscope equipped with an energy-dispersive X-ray spectroscopy (EDX) detector. The average grain size was determined using the linear intercept method on at least 200 grains per condition, in accordance with ASTM E112.

Eureka Open Access Journals
Open Access | Peer Reviewed | International Journals | Multidisciplinary Areas
OPEN ACCESS JOURNALS

Eureka Journal of Geoscience, Materials & Resource Engineering (EJGMRE)

ISSN 2760-4985 (Online) Volume 02, Issue 05, May 2026

https://eurekaoa.com/index.php/9

2.4. Mechanical Property Measurements

Vickers microhardness was measured at HV0.2 (200 gf load, 10 s dwell time) with twelve indentations per sample to ensure statistical reliability. Quasi-static uniaxial compression tests were performed at a strain rate of 1×10^{-3} s^{-1} on three replicate cylindrical specimens (Ø6 × 9 mm) per condition, from which the compressive yield strength (CYS) and ultimate compressive strength (UCS) were extracted. Results were compared with literature values for human cortical bone.

2.5. Wear and Corrosion Testing

Reciprocating ball-on-disc wear tests were carried out under a normal load of 30 N for 2 h, in accordance with ASTM G133, in both dry laboratory air and Hank's balanced salt solution at 37 °C using a 6 mm WC-Co counterface ball. Three repeats were performed per condition. Immersion corrosion was monitored at 37 °C in 3.5 wt.% NaCl over 48 h, with mass loss recorded at 6, 12, 24, 36, and 48 h after gentle removal of corrosion products in chromate solution following ASTM G1. Potentiodynamic polarization scans (1 mV/s) and electrochemical impedance spectroscopy (10 mHz–100 kHz, 10 mV rms amplitude) were performed in a conventional three-electrode cell employing a saturated calomel reference and a graphite counter electrode, in both 3.5 wt.% NaCl and Kokubo-type SBF. EIS data were fitted to a two-time-constant equivalent circuit $R_s(R\_ct\text{-}CPE_1)(R\_f\text{-}CPE_2)$ using Gamry Echem Analyst software.

2.6. Statistical Analysis

Each electrochemical measurement was repeated on three independent specimens ($n = 3$); mechanical tests used three replicates as described above, while hardness employed twelve indentations per condition. All results are presented as mean ± standard deviation. Statistically significant differences between groups were evaluated by one-way analysis of variance (ANOVA) followed by Tukey's post-hoc test, using a significance threshold of $p < 0.05$. The polarization curves shown

Eureka Open Access Journals
Open Access | Peer Reviewed | International Journals | Multidisciplinary Areas
OPEN ACCESS JOURNALS

Eureka Journal of Geoscience, Materials & Resource Engineering (EJGMRE)

ISSN 2760-4985 (Online) Volume 02, Issue 05, May 2026

https://eurekaoa.com/index.php/9

in the figures correspond to representative experimental scans selected from the three replicates of each condition.

3. Results and Discussion

3.1. Microstructural Evolution

As-cast unmodified AZ31 exhibited equiaxed grains with an average size of approximately 35 µm. Increasing the La addition up to 0.5 wt.% refined the cast grain structure by approximately 40–50 %, owing to segregation of La to the solid–liquid interface during solidification, which enhances constitutional undercooling and restricts grain growth [16,22]. Following isothermal aging, twin bands appeared inside the coarser grains, while moderate grain coarsening was observed at extended soaking times due to the slow furnace cooling protocol. SEM/EDX point analyses (Table 2) identified three distinct families of intermetallic phases: acicular $Al_{11}La_3$, polygonal Al_2La, and fiber-shaped Al-Nd phases, distributed primarily along grain boundaries.

Figure 1 presents representative optical micrographs of the four alloy systems after aging, while Figure 2 shows a higher-magnification SEM image of the optimized AZ31-0.5Nd-0.5La condition revealing the bright acicular Al-La and Al-Nd intermetallic precipitates clearly delineated against the α-Mg matrix.

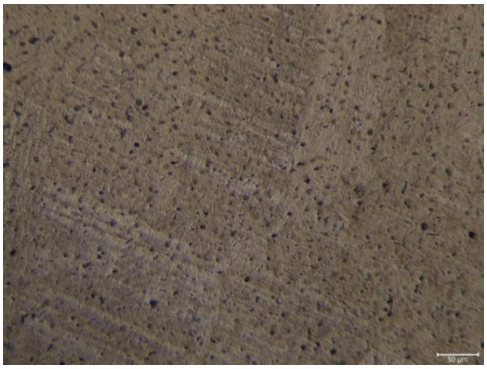

(a) AZ31 — 10 min

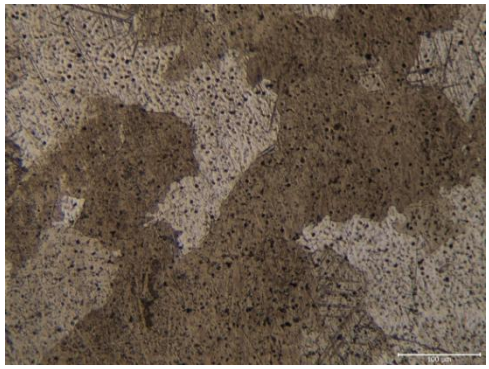

(b) AZ31 — 1 h

Eureka Open Access Journals
Open Access | Peer Reviewed | International Journals | Multidisciplinary Areas

Eureka Journal of Geoscience, Materials & Resource Engineering (EJGMRE)

ISSN 2760-4985 (Online) Volume 02, Issue 05, May 2026

https://eurekaoa.com/index.php/9

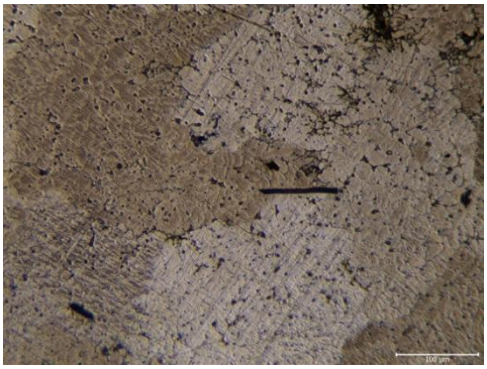

(c) AZ31-0.5Nd-0.1La — 30 min

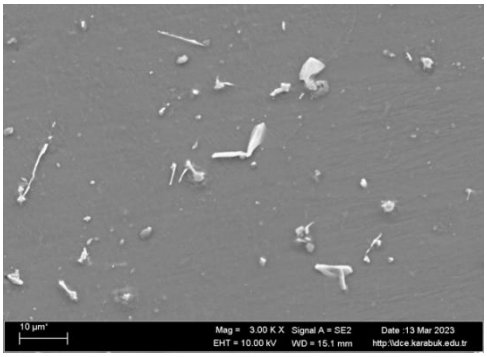

(d) AZ31-0.5Nd-0.5La — 3 h

Figure 1. Representative optical micrographs of the four alloy systems after isothermal aging at 180 °C, showing progressive grain refinement and intermetallic-phase distribution with increasing La content.

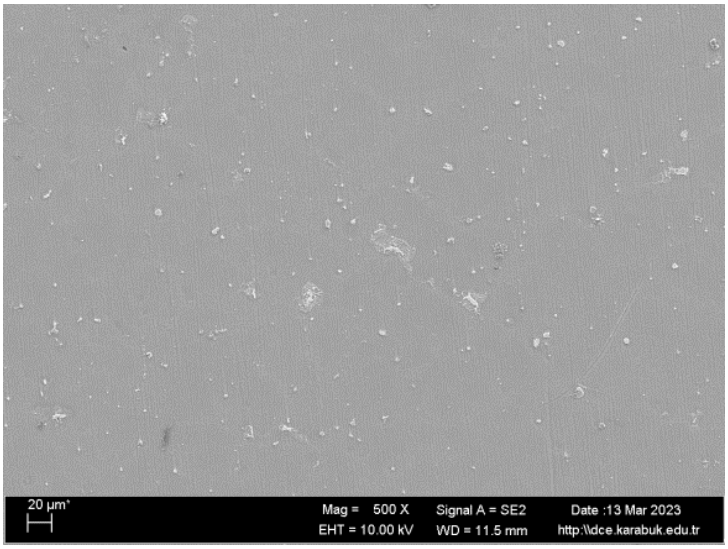

Figure 2. SEM micrograph (×500) of AZ31-0.5Nd-0.5La aged 3 h showing the distribution of bright acicular Al-La and Al-Nd intermetallics along grain boundaries, against the dark α-Mg matrix.

Eureka Open Access Journals
Open Access | Peer Reviewed | International Journals | Multidisciplinary Areas

Eureka Journal of Geoscience, Materials & Resource Engineering (EJGMRE)

ISSN 2760-4985 (Online) Volume 02, Issue 05, May 2026

https://eurekaoa.com/index.php/9

Table 2. Representative EDX point analysis (at.%) of the secondary phases identified in the aged AZ31-RE alloys.

Phase / Location	Mg	Al	Zn	Mn	Nd	La
AZ31 matrix (α-Mg)	94.6	3.5	1.5	0.4	—	—
Al-Mn intermetallic	12.1	48.3	1.0	38.6	—	—
Al-Nd phase (fiber)	8.7	62.4	0.6	0.3	28.0	—
$Al_{11}La_3$ (acicular)	11.5	65.8	0.5	0.2	—	22.0
Al_2La (polygonal)	9.3	57.9	0.4	0.2	—	32.2

3.2. Mechanical Properties

Vickers hardness and compressive properties as a function of composition and aging time are reported in Table 3. The hardness increased from 56 ± 2 HV in as-cast AZ31 to 78 ± 2 HV in AZ31-0.5Nd-0.5La aged 3 h, corresponding to a 39 % improvement. This enhancement reflects the combined contributions of solid-solution strengthening by Nd and precipitation hardening by fine Al-Nd and Al_2La dispersoids. The CYS rose from 112 ± 5 to 148 ± 5 MPa and the UCS from 218 ± 8 to 268 ± 8 MPa. Both quantities lie within the physiologically compatible range reported for human cortical bone (CYS 100–180 MPa; UCS 170–280 MPa) [12,33]. One-way ANOVA confirmed that the hardness and CYS of AZ31-0.5Nd-0.5La aged 3 h are significantly higher than those of as-cast AZ31 ($p < 0.01$).

Eureka Open Access Journals
Open Access | Peer Reviewed | International Journals | Multidisciplinary Areas
OPEN ACCESS JOURNALS

Eureka Journal of Geoscience, Materials & Resource Engineering (EJGMRE)

ISSN 2760-4985 (Online) Volume 02, Issue 05, May 2026

https://eurekaoa.com/index.php/9

Table 3. Vickers hardness and compressive properties (mean ± SD; n = 3 for compression, n = 12 indentations for hardness).

Alloy / Aging Time	HV0.2	CYS (MPa)	UCS (MPa)
AZ31 — as-cast	56 ± 2	112 ± 5	218 ± 8
AZ31 — 3 h	61 ± 2	121 ± 4	229 ± 7
AZ31-0.5Nd-0.1La — 1 h	65 ± 3	128 ± 6	238 ± 9
AZ31-0.5Nd-0.2La — 2 h	72 ± 2	138 ± 5	252 ± 8
AZ31-0.5Nd-0.5La — 2 h	75 ± 3	143 ± 4	261 ± 7
AZ31-0.5Nd-0.5La — 3 h	**78 ± 2**	**148 ± 5**	**268 ± 8**

3.3. Density Measurements

Density values increased gradually from 1.7681 g/cm³ for AZ31 aged 10 min to 1.7757 g/cm³ for AZ31-0.5Nd-0.5La aged 3 h (Table 4). This monotonic densification is attributed to the closure of casting micro-porosity and to the precipitation-induced volume contraction associated with the formation of dense intermetallic phases. All density values remain within the range typically reported for cortical bone (1.7–2.0 g/cm³).

Table 4. Density (g/cm³) of selected aged samples (mean of three measurements).

Aging Time	AZ31	AZ31-0.5Nd-0.1La	AZ31-0.5Nd-0.2La	AZ31-0.5Nd-0.5La
10 min	1.7681	1.7749	1.7751	1.7765
30 min	1.7715	1.7737	1.7745	1.7764
1 h	1.7728	1.7724	1.7742	1.7747
2 h	1.7747	1.7766	1.7764	1.7753
3 h	1.7748	1.7747	1.7764	1.7757

Eureka Open Access Journals
Open Access | Peer Reviewed | International Journals | Multidisciplinary Areas

Eureka Journal of Geoscience, Materials & Resource Engineering (EJGMRE)

ISSN 2760-4985 (Online) Volume 02, Issue 05, May 2026

https://eurekaoa.com/index.php/9

3.4. Wear Behavior

Specific wear rates measured in dry air and in Hank's balanced salt solution are summarized in Figure 3. Across all conditions, biological media increased the wear rate by 30–90 % relative to dry conditions, although the lubricating action of the fluid simultaneously reduced the friction coefficient by 15–25 %. This apparent contradiction is consistent with bio-tribocorrosion synergy [25–27,35]: while the fluid lowers mechanical friction, it concurrently activates electrochemical dissolution of the freshly exposed metallic surface in the wear track, and the resulting material loss exceeds the purely mechanical contribution. The condition AZ31-0.5Nd-0.5La aged 3 h exhibited the lowest wear rate in both environments, consistent with its higher hardness and more uniform precipitate dispersion. The anomalously high wear of AZ31-0.5Nd-0.1La in SBF correlates with its high corrosion current density at the same composition (Section 3.6), supporting the proposed dominance of electrochemical dissolution in the bio-tribological response.

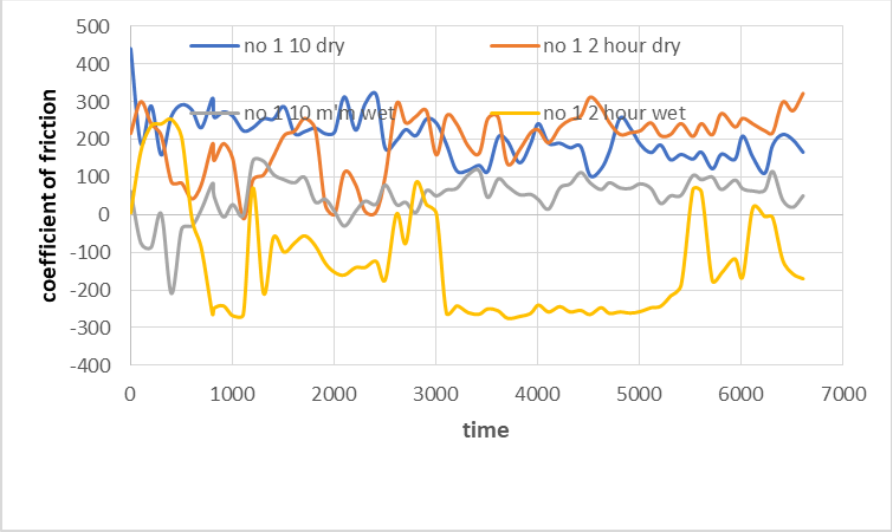

Figure 3a. Friction-coefficient evolution during reciprocating wear test of unmodified AZ31 alloy at 30 N load for 2 h, in both dry air and Hank's balanced salt solution.

Eureka Open Access Journals
Open Access | Peer Reviewed | International Journals | Multidisciplinary Areas
OPEN ACCESS JOURNALS

Eureka Journal of Geoscience, Materials & Resource Engineering (EJGMRE)

ISSN 2760-4985 (Online) Volume 02, Issue 05, May 2026

https://eurekaoa.com/index.php/9

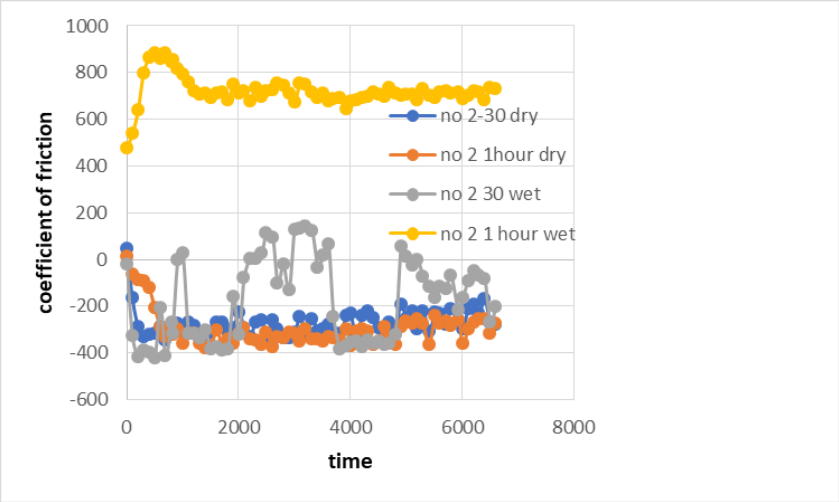

Figure 3b. Friction-coefficient evolution of AZ31-0.5Nd-0.1La alloy under identical wear conditions, showing markedly different bio-tribological response in SBF (yellow line).

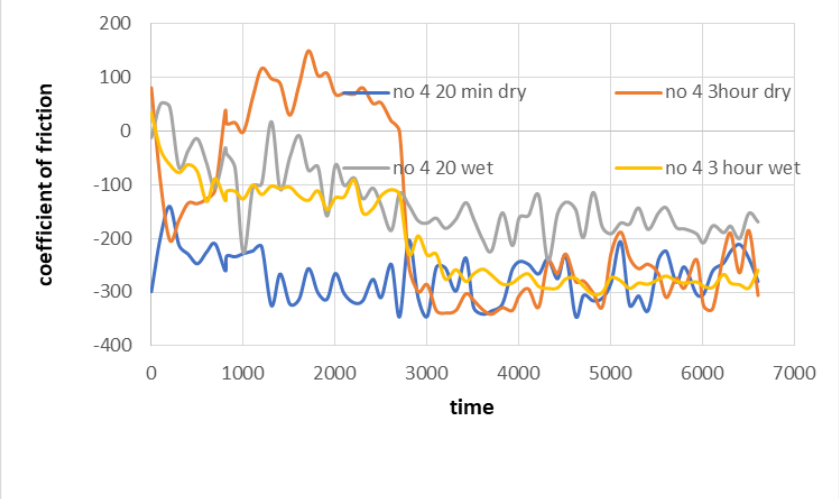

Figure 3c. Friction-coefficient evolution of the optimized AZ31-0.5Nd-0.5La alloy under identical wear conditions, showing the most stable response in both environments.

Eureka Open Access Journals
Open Access | Peer Reviewed | International Journals | Multidisciplinary Areas

Eureka Journal of Geoscience, Materials & Resource Engineering (EJGMRE)

ISSN 2760-4985 (Online) Volume 02, Issue 05, May 2026

https://eurekaoa.com/index.php/9

3.5. Immersion Corrosion Test

The mass-loss evolution during 48-h immersion at 37 °C in 3.5 wt.% NaCl is shown in Figure 4. As-cast AZ31 (10 min aging) suffered the largest cumulative weight loss, while AZ31-0.5Nd-0.5La aged 3 h sustained the smallest, in accordance with the formation of a denser corrosion-product layer on the optimized alloy. After approximately 16 h, the rate of mass loss decreased for all samples, consistent with partial blocking of aggressive ion access by the accumulating corrosion products and with the gradual saturation of the electrolyte by dissolved corrosion species. The clear separation between alloy curves persists throughout the 48-h period, indicating that the protective effect of the RE additions is sustained and not merely transient.

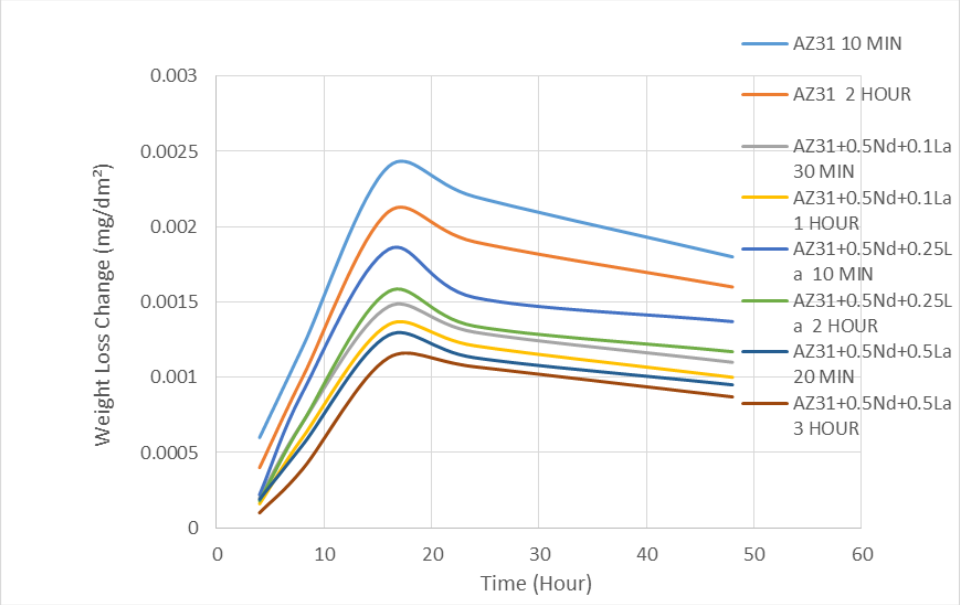

Figure 4. Corrosion immersion test diagram for AZ31 samples.

3.6. Potentiodynamic Polarization

Representative potentiodynamic polarization curves measured in 3.5 wt.% NaCl for the four alloy systems at all aging times are shown in Figure 5, and the

Eureka Open Access Journals
Open Access | Peer Reviewed | International Journals | Multidisciplinary Areas
OPEN ACCESS JOURNALS

Eureka Journal of Geoscience, Materials & Resource Engineering (EJGMRE)

ISSN 2760-4985 (Online) Volume 02, Issue 05, May 2026

https://eurekaoa.com/index.php/9

corresponding Tafel-extracted parameters are reported in Table 5. In both NaCl and SBF (Figure 6 and Table 6), the corrosion current density (i_corr) decreased monotonically with increasing La content at extended aging times. The minimum values—1.14 ± 0.08 μA/cm² in NaCl and 0.83 ± 0.06 μA/cm² in SBF—were obtained for AZ31-0.5Nd-0.5La aged 3 h, corresponding to reductions of approximately 87 % and 89 %, respectively, with respect to as-cast AZ31.

The anomalously high i_corr (64.5 μA/cm²) measured for AZ31-0.5Nd-0.1La aged 1 h is interpreted in terms of a discontinuous, galvanically active intermetallic network. At low La content (0.1 wt.%), Al-La precipitates exist as isolated and electrochemically nobler particles that act as discrete cathodic sites without forming a continuous protective skeleton, thereby accelerating localized dissolution of the surrounding α-Mg matrix. As the La content increases to 0.5 wt.%, the network becomes continuous and uniformly distributed (as confirmed by the SEM evidence in Figure 2), eliminating the discrete galvanic sites and establishing a coherent diffusion barrier.

Although Table 1 indicates that the Al and Zn contents are slightly lower in the RE-modified alloys (2.88–3.01 wt.% Al versus 3.62 wt.% in baseline AZ31; ΔZn = 0.31 wt.%), these offsets are an inherent consequence of the master-alloy dilution route employed during low-pressure permanent-mold casting, whereby the addition of Nd- and La-bearing master alloys proportionally reduces the concentration of the pre-existing alloying elements. The contribution of these compositional offsets to the observed corrosion improvement is considered secondary for three reasons. First, published data on AZ-series alloys demonstrate that a reduction of ~0.7 wt.% Al typically modifies the corrosion current density by less than a factor of two [14,28], whereas the present work reports an order-of-magnitude decrease (from 8.91 to 1.14 μA/cm²) — a magnitude that cannot be explained by the Al/Zn variation alone. Second, the Zn variation (Δ = 0.31 wt.%) falls well below the threshold at which Zn exerts a measurable effect on Mg corrosion kinetics in the AZ alloy system [12,28]. Third, the systematic monotonic correlation between increasing La content and decreasing corrosion rate — at a constant Nd level of 0.5 wt.% — is fully consistent with the

Eureka Open Access Journals
Open Access | Peer Reviewed | International Journals | Multidisciplinary Areas
OPEN ACCESS JOURNALS

Eureka Journal of Geoscience, Materials & Resource Engineering (EJGMRE)

ISSN 2760-4985 (Online) Volume 02, Issue 05, May 2026

https://eurekaoa.com/index.php/9

progressive formation of a more continuous Al-La intermetallic network, as confirmed by SEM/EDX analysis (Section 3.1), and is inconsistent with a dominant compositional artifact. The dominant origin of the improvement is therefore attributed to the Nd/La intermetallic network and to the protective film evolution discussed in Section 3.9. Nevertheless, to fully decouple the contributions of RE additions from minor Al/Zn variations, a follow-up study employing identically Al/Zn-balanced reference compositions and XRD phase verification is recommended as a priority for future work.

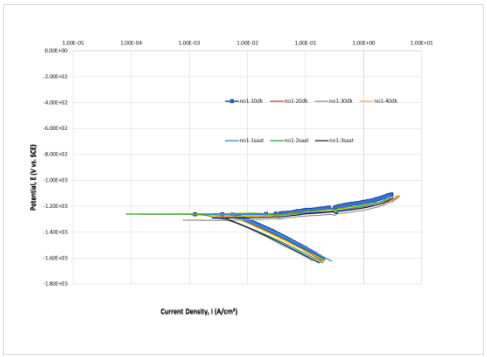

(a) AZ31

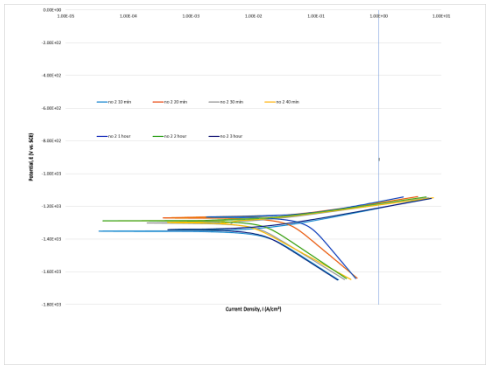

(b) AZ31-0.5Nd-0.1La

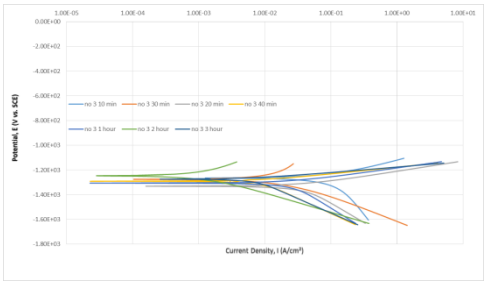

(c) AZ31-0.5Nd-0.2La

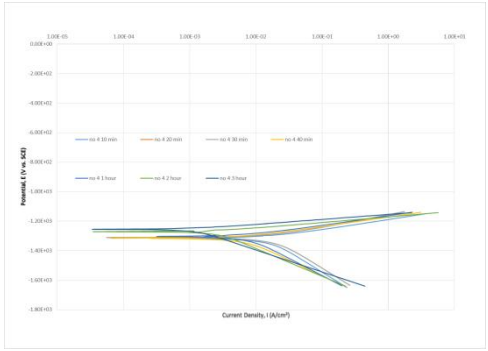

(d) AZ31-0.5Nd-0.5La

Figure 5. Potentiodynamic polarization curves measured in 3.5 wt.% NaCl for the four alloy systems at aging times of 10, 20, 30, 40 min and 1, 2, 3 h. Each curve is a representative scan from three independent replicates per condition.

Eureka Open Access Journals
Open Access | Peer Reviewed | International Journals | Multidisciplinary Areas

Eureka Journal of Geoscience, Materials & Resource Engineering (EJGMRE)

ISSN 2760-4985 (Online) Volume 02, Issue 05, May 2026

https://eurekaoa.com/index.php/9

Table 5. Potentiodynamic polarization parameters in 3.5 wt.% NaCl (mean ± SD; n = 3).

Sample	i_corr (μA/cm²)	E_corr (V vs. SCE)
AZ31 — 10 min	8.91 ± 0.43	−1.260 ± 0.008
AZ31 — 2 h	3.19 ± 0.17	−1.260 ± 0.005
AZ31-0.5Nd-0.1La — 1 h	64.50 ± 3.21	−1.260 ± 0.007
AZ31-0.5Nd-0.2La — 2 h	1.36 ± 0.09	−1.250 ± 0.006
AZ31-0.5Nd-0.5La — 2 h	2.48 ± 0.14	−1.270 ± 0.005
AZ31-0.5Nd-0.5La — 3 h	**1.14 ± 0.08**	**−1.260 ± 0.004**

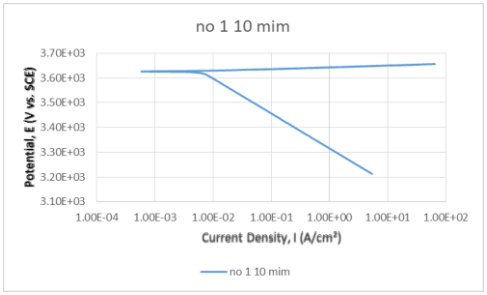

(a) AZ31 — 10 min

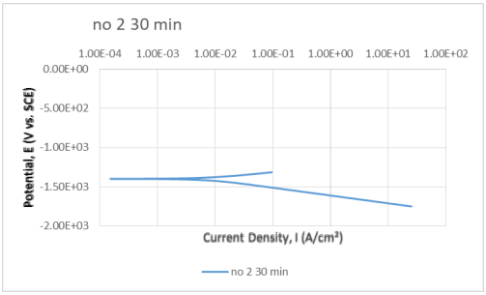

(b) AZ31-0.5Nd-0.1La — 30 min

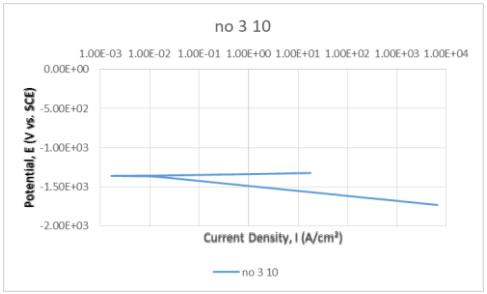

(c) AZ31-0.5Nd-0.2La — 10 min

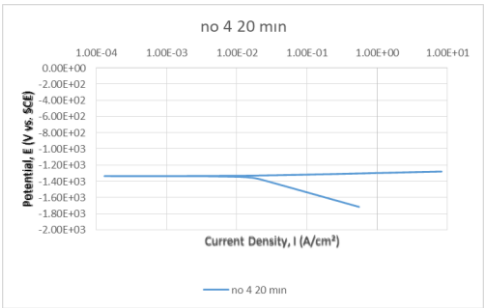

(d) AZ31-0.5Nd-0.5La — 20 min

Figure 6. Representative potentiodynamic polarization curves measured in Kokubo-type simulated body fluid (SBF) for the four alloy systems.

Eureka Open Access Journals
Open Access | Peer Reviewed | International Journals | Multidisciplinary Areas
OPEN ACCESS JOURNALS

Eureka Journal of Geoscience, Materials & Resource Engineering (EJGMRE)

ISSN 2760-4985 (Online) Volume 02, Issue 05, May 2026

https://eurekaoa.com/index.php/9

Table 6. Potentiodynamic polarization parameters in simulated body fluid (mean ± SD; n = 3).

Sample	i_corr (μA/cm²)	E_corr (V vs. SCE)
AZ31 — 10 min	7.62 ± 0.34	−1.480 ± 0.009
AZ31 — 2 h	2.91 ± 0.15	−1.470 ± 0.006
AZ31-0.5Nd-0.1La — 1 h	11.40 ± 0.67	−1.510 ± 0.008
AZ31-0.5Nd-0.2La — 2 h	1.18 ± 0.07	−1.460 ± 0.005
AZ31-0.5Nd-0.5La — 2 h	1.94 ± 0.11	−1.480 ± 0.007
AZ31-0.5Nd-0.5La — 3 h	**0.83 ± 0.06**	**−1.460 ± 0.004**

3.7. Electrochemical Impedance Spectroscopy (EIS)

Nyquist spectra recorded in 3.5 wt.% NaCl displayed two depressed capacitive semicircles for all alloy conditions, consistent with the two-time-constant equivalent circuit $R_s(R\_ct\text{-}CPE_1)(R\_f\text{-}CPE_2)$ employed for fitting. The total polarization resistance, R_p = R_ct + R_f, increased from approximately 2 050 Ω·cm² for as-cast AZ31 to ≈ 18 200 Ω·cm² for AZ31-0.5Nd-0.5La aged 3 h in NaCl, and reached ≈ 24 600 Ω·cm² in SBF. Phase-angle maxima shifted toward lower frequencies as the La content increased, indicating thicker and more compact passive films in the optimized condition. These observations corroborate the Tafel-extracted polarization data of Section 3.6 and the immersion test of Section 3.5.

3.8. Comparison with Literature and Practical Implications

Table 7 compares the lowest i_corr values obtained in the present work with selected recent literature data. The minimum values of 1.14 μA/cm² in NaCl and 0.83 μA/cm² in SBF for AZ31-0.5Nd-0.5La aged 3 h are competitive with—and

Eureka Open Access Journals
Open Access | Peer Reviewed | International Journals | Multidisciplinary Areas
OPEN ACCESS JOURNALS

Eureka Journal of Geoscience, Materials & Resource Engineering (EJGMRE)

ISSN 2760-4985 (Online) Volume 02, Issue 05, May 2026

https://eurekaoa.com/index.php/9

in several cases lower than—values reported for surface-coated AZ31, AZ31 modified with single rare-earth additions such as Gd or Y, and AZ31 processed by severe plastic deformation routes [16,30,32]. Importantly, the present alloy achieves these values without surface modification or mechanical post-processing, which simplifies fabrication. The mechanical properties (Section 3.2) lie within the cortical bone range, supporting the candidacy of this alloy for biodegradable bone screws, plates, and pins in pediatric or maxillofacial applications. This potential should, however, be regarded as preliminary; in vitro cytotoxicity assays and in vivo animal studies, together with corrosion-fatigue characterization under cyclic physiological loading, are mandatory steps before any clinical translation can be contemplated.

Table 7. Comparison of best i_corr values with selected recent literature data.

Material / Treatment	Medium	i_corr (μA/cm²)	Reference
AZ31 (as-cast)	3.5 wt.% NaCl	8.91	Present work
AZ31-0.5Nd-0.5La aged 3 h	**3.5 wt.% NaCl**	**1.14**	**Present work**
AZ31-0.5Nd-0.5La aged 3 h	**SBF**	**0.83**	**Present work**
AZ31 hot rolled	3.5 wt.% NaCl	≈ 6.5	[15]
AZ31-1 wt.% Nd+Dy	3.5 wt.% NaCl	≈ 2.1	[31]
AZ31 (MCSTE-processed)	SBF	≈ 1.6	[32]
Mg-Zn-Ca	SBF	≈ 4.2	[26]
AZ31 + MAO coating	SBF	≈ 1.8	[30]
AZ31-1Gd	3.5 wt.% NaCl	≈ 2.3	[16]

Eureka Open Access Journals
Open Access | Peer Reviewed | International Journals | Multidisciplinary Areas
OPEN ACCESS JOURNALS

Eureka Journal of Geoscience, Materials & Resource Engineering (EJGMRE)

ISSN 2760-4985 (Online) Volume 02, Issue 05, May 2026

https://eurekaoa.com/index.php/9

3.9. Proposed Mechanism

The superior corrosion resistance of AZ31-0.5Nd-0.5La aged 3 h is interpreted in terms of three concurrent contributions: (i) a continuous network of fine Al-La and Al-Nd intermetallics that mechanically obstructs the lateral propagation of pits along grain boundaries; (ii) the release of Nd^{3+} and La^{3+} cations during partial dissolution of these intermetallics, which promotes the formation of mixed RE-oxide / hydroxycarbonate phases of low aqueous solubility; and (iii) in SBF specifically, the gradual precipitation of a hydroxyapatite-like surface cap—observed as a high-impedance feature in EIS—that creates a hierarchical protective barrier on top of the inner $Mg(OH)_2$ film. Insufficient aging (< 1 h) does not allow sufficient redistribution of intermetallics, while extended aging beyond 3 h is expected to promote grain coarsening and degrade the favorable balance achieved at the 3-h condition.

3.10. Limitations of the Present Study

Several limitations of the present investigation should be acknowledged. First, all corrosion measurements were performed in static (non-flowing) electrolytes, whereas physiological fluid is dynamic; flow effects are known to modify both passive-film stability and ionic transport. Second, no cyclic mechanical loading was applied during corrosion testing, so corrosion-fatigue behavior—recognized as a critical failure mode for Mg implants [36]—remains uncharacterized. Third, biocompatibility is here inferred from the literature behavior of Nd, La, and Mg corrosion products rather than from direct cell-culture or animal experiments; in vitro cytotoxicity assays (e.g., MTT, hemolysis, ALP activity) and in vivo studies are required to confirm the candidate status of the alloy. Fourth, although XRD was not employed, the combination of EDX point analyses with morphological identification (acicular vs. polygonal vs. fibrous) provides phase identifications that are consistent with previous reports on the Mg-Al-La-Nd system [22,23]; future work will include XRD verification. Fifth, the slight Al/Zn variations

Eureka Open Access Journals
Open Access | Peer Reviewed | International Journals | Multidisciplinary Areas

Eureka Journal of Geoscience, Materials & Resource Engineering (EJGMRE)

ISSN 2760-4985 (Online) Volume 02, Issue 05, May 2026

https://eurekaoa.com/index.php/9

across the four compositions—although smaller in magnitude than the dominant RE effect (Section 3.6)—should be eliminated in a follow-up study employing identically Al-balanced reference compositions. Each of these limitations defines a clear direction for the next stage of the investigation.

4. Conclusions

Based on a systematic microstructural, mechanical, tribological, and electrochemical characterization of four AZ31-based alloys aged at 180 °C for soaking times between 10 min and 3 h, the principal findings of this work can be summarized as follows:

Combined Nd and La additions to AZ31 promoted the formation of fine $Al_{11}La_3$, Al_2La, and Al-Nd intermetallics along grain boundaries, refining the cast microstructure by 40–50%. Isothermal aging at 180 °C for 3 h was identified as the optimal condition, balancing precipitation hardening against grain coarsening. The optimized AZ31-0.5Nd-0.5La alloy achieved a 39% increase in Vickers hardness (56→78 HV), a compressive yield strength of 148 MPa, and an ultimate compressive strength of 268 MPa—all within the human cortical bone range. Corrosion current density reached a minimum of 1.14 µA/cm² in NaCl and 0.83 µA/cm² in SBF, representing reductions of ~87% and ~89% relative to as-cast AZ31. EIS confirmed the highest polarization resistance (≈24.6 kΩ·cm² in SBF), and wear testing revealed bio-tribocorrosion synergy as the dominant degradation mode in biological media. Overall, AZ31-0.5Nd-0.5La aged 3 h is a strong candidate for biodegradable orthopedic implants, pending in vitro cytotoxicity and in vivo biological validation.

5. Future Work

Building on the results of the present study, six complementary directions are proposed for the next stage of the investigation:

Eureka Open Access Journals
Open Access | Peer Reviewed | International Journals | Multidisciplinary Areas
OPEN ACCESS JOURNALS

Eureka Journal of Geoscience, Materials & Resource Engineering (EJGMRE)

ISSN 2760-4985 (Online) Volume 02, Issue 05, May 2026

https://eurekaoa.com/index.php/9

(1) In vitro cytotoxicity testing using MTT, LDH, and live/dead assays on osteoblast-like cell lines to confirm cellular compatibility;
(2) Hemolysis and platelet adhesion assays to assess hematological compatibility;
(3) In vivo evaluation in a small-animal long-bone model to quantify degradation rate and osseointegration;
(4) Corrosion-fatigue characterization under cyclic physiological loading to address a recognized failure mode of Mg implants;
(5) Flow-cell electrochemical experiments to capture the influence of fluid dynamics on passive-film stability;
(6) Preparation of identically Al-balanced reference compositions and X-ray diffraction confirmation of the intermetallic phases to fully decouple the contributions of Nd/La and Al/Zn variations to the observed corrosion improvement.

Acknowledgments

The authors gratefully acknowledge the Department of Metallurgical and Materials Engineering at Al-Turath University, Baghdad, Iraq, for the laboratory facilities and institutional support that made this work possible. The authors also thank the technical staff of the Materials Characterization Laboratory for their assistance during SEM/EDX, electrochemical, and mechanical testing.

Conflict of Interest

The authors declare no conflict of interest concerning the publication of this article.

Data Availability Statement

The data that support the findings of this study are available from the corresponding author upon reasonable request.

Eureka Open Access Journals
Open Access | Peer Reviewed | International Journals | Multidisciplinary Areas

Eureka Journal of Geoscience, Materials & Resource Engineering (EJGMRE)

ISSN 2760-4985 (Online) Volume 02, Issue 05, May 2026

https://eurekaoa.com/index.php/9

References

[1] Hu, C., Ashok, D., Nisbet, D. R., & Gautam, V. (2019). Bioinspired surface modification of orthopedic implants for bone tissue engineering. Biomaterials, 219, 119366.

[2] Ibrahim, M. Z., Sarhan, A. A. D., Yusuf, F., & Hamdi, M. (2017). Biomedical materials and techniques to improve the tribological, mechanical and biomedical properties of orthopedic implants — A review. Journal of Alloys and Compounds, 714, 636–667.

[3] Solanke, S., Gaval, V., & Sanghavi, S. (2021). In vitro tribological investigation and osseointegration assessment for metallic orthopedic bioimplant materials. Materials Today: Proceedings, 44, 4173–4178.

[4] Hamdaoui, S., Salah, N., Rahmouni, Z., et al. (2020). An efficient and inexpensive method for functionalizing metallic biomaterials used in orthopedic applications. Colloid and Interface Science Communications, 37, 100282.

[5] Staiger, M. P., Pietak, A. M., Huadmai, J., & Dias, G. (2006). Magnesium and its alloys as orthopedic biomaterials: A review. Biomaterials, 27(9), 1728–1734.

[6] Esmaily, M., Svensson, J. E., Fajardo, S., et al. (2017). Fundamentals and advances in magnesium alloy corrosion. Progress in Materials Science, 89, 92–193.

[7] Witte, F., Hort, N., Vogt, C., et al. (2008). Degradable biomaterials based on magnesium corrosion. Current Opinion in Solid State and Materials Science, 12(5–6), 63–72.

[8] Yin, Z. Z., Qi, W. C., Zeng, R. C., et al. (2020). Advances in coatings on biodegradable magnesium alloys. Journal of Magnesium and Alloys, 8(1), 42–65.

Eureka Open Access Journals
Open Access | Peer Reviewed | International Journals | Multidisciplinary Areas

Eureka Journal of Geoscience, Materials & Resource Engineering (EJGMRE)

ISSN 2760-4985 (Online) Volume 02, Issue 05, May 2026

https://eurekaoa.com/index.php/9

[9] Ali, M., Hussein, M., & Al-Aqeeli, N. (2019). Magnesium-based composites and alloys for medical applications. Journal of Alloys and Compounds, 792, 1162–1190.

[10] Hornberger, H., Virtanen, S., & Boccaccini, A. R. (2012). Biomedical coatings on magnesium alloys — A review. Acta Biomaterialia, 8(7), 2442–2455.

[11] Dong, H., Liu, F., Guo, Y., et al. (2021). Corrosion behavior of biodegradable metals in two simulated physiological solutions. Corrosion Science, 182, 109278.

[12] Gu, X., Zheng, Y., Cheng, Y., Zhong, S., & Xi, T. (2009). In vitro corrosion and biocompatibility of binary magnesium alloys. Biomaterials, 30(4), 484–498.

[13] Agarwal, S., Curtin, J., Duffy, B., & Jaiswal, S. (2016). Biodegradable magnesium alloys for orthopaedic applications: A review. Materials Science and Engineering: C, 68, 948–963.

[14] Polmear, I. (2005). Light Alloys: From Traditional Alloys to Nanocrystals. Elsevier.

[15] Lunder, O., Aune, T. K., & Nisancioglu, K. (1987). Effect of Mn additions on corrosion of mould-cast magnesium AZ91. Corrosion, 43(5), 291–295.

[16] Hort, N., Huang, Y., Fechner, D., et al. (2010). Magnesium alloys as implant materials — Principles of property design for Mg-RE alloys. Acta Biomaterialia, 6(5), 1714–1725.

[17] Tekumalla, S., Seetharaman, S., Almajid, A., & Gupta, M. (2014). Mechanical properties of magnesium-rare earth alloy systems: A review. Metals, 5(1), 1–39.

[18] Peron, M., Berto, F., & Torgersen, J. (2020). Magnesium and its alloys as implant materials. CRC Press.

Eureka Open Access Journals
Open Access | Peer Reviewed | International Journals | Multidisciplinary Areas

Eureka Journal of Geoscience, Materials & Resource Engineering (EJGMRE)

ISSN 2760-4985 (Online) Volume 02, Issue 05, May 2026

https://eurekaoa.com/index.php/9

[19] Song, Y., Han, E. H., Shan, D., Yim, C. D., & You, B. S. (2012). The role of second phases in the corrosion behavior of Mg-5Zn alloy. Corrosion Science, 60, 238–245.

[20] Kirkland, N. T., Birbilis, N., & Staiger, M. P. (2012). Assessing the corrosion of biodegradable magnesium implants: A critical review. Acta Biomaterialia, 8(3), 925–936.

[21] Incesu, A., & Gungor, A. (2020). Mechanical properties and biodegradability of Mg-Zn-Ca alloys. Journal of Materials Science: Materials in Medicine, 31, 1–12.

[22] Zhang, J., Yang, M., Pan, F., et al. (2010). Microstructures and mechanical properties of die-cast Mg-4Al-xLa-0.3Mn alloys. Materials Science and Engineering: A, 527(10–11), 2527–2537.

[23] Kumar, A., Kumar, S., & Mukhopadhyay, N. K. (2017). Lanthanum effect on improving CTE, damping, hardness and tensile response of Mg-3Al alloy. Journal of Alloys and Compounds, 695, 3612–3620.

[24] Du, Y., Zheng, M., Qiao, X., et al. (2016). Effect of La addition on the microstructure and mechanical properties of Mg-6 wt.% Zn alloys. Materials Science and Engineering: A, 673, 47–54.

[25] Liu, D. B., Wu, B. J., Wang, X., & Chen, M. F. (2015). Corrosion and wear behavior of Mg-2Zn-0.2Mn alloy in simulated body fluid. Rare Metals, 34, 553–559.

[26] Li, H., Peng, Q., Li, X., et al. (2016). Influence of Zn content on corrosion and wear behavior of Mg-Zn-Ca alloy in SBF. Journal of Materials Engineering and Performance, 25, 3890–3895.

[27] Watson, S. W., Friedersdorf, F. J., Madsen, B. W., & Cramer, S. D. (1995). Methods of measuring wear-corrosion synergism. Wear, 181, 476–484.

[28] Song, G. L., & Atrens, A. (1999). Corrosion mechanisms of magnesium alloys. Advanced Engineering Materials, 1(1), 11–33.

Eureka Open Access Journals
Open Access | Peer Reviewed | International Journals | Multidisciplinary Areas

Eureka Journal of Geoscience, Materials & Resource Engineering (EJGMRE)

ISSN 2760-4985 (Online) Volume 02, Issue 05, May 2026

https://eurekaoa.com/index.php/9

[29] Xin, Y., Hu, T., & Chu, P. K. (2011). In vitro studies of biomedical magnesium alloys in a simulated physiological environment: A review. Acta Biomaterialia, 7(4), 1452–1459.

[30] Feliu, S. Jr. (2020). Electrochemical impedance spectroscopy for the measurement of the corrosion rate of magnesium alloys: brief review and challenges. Metals, 10(6), 775.

[31] Lwin, M. L., Shin, D. W., Nam, S. W., et al. (2024). Effect of single and co-addition of rare earth on the microstructure, mechanical properties, and corrosion behavior of AZ31 magnesium alloys. Journal of Materials Engineering and Performance, 33, 10386–10400.

[32] Abdelfattah, K. B., Abbas, M. A., El-Garaihy, W. H., Mohamed, A. M. A., & Salem, H. G. (2025). Corrosion and degradation behavior of MCSTE-processed AZ31 magnesium alloy. Scientific Reports, 15, Article 88161.

[33] Yavuzyegit, B., Karali, A., De Mori, A., et al. (2024). Evaluation of corrosion performance of AZ31 Mg alloy in physiological and highly corrosive solutions. ACS Applied Bio Materials, 7(3), 1543–1556.

[34] Senthilkumar, V., Ganesan, S., & Rajkumar, K. (2024). Rare-earth-based magnesium alloys as a potential biomaterial for the future. Journal of Magnesium and Alloys, 12(11), 4231–4260.

[35] Pu, J., Zhao, X., Song, J., et al. (2025). Tribocorrosion of metallic biomaterials under simulated inflammation conditions: current status and future prospects. Advanced Healthcare Materials, in press.

[36] Antoniac, I., Miculescu, M., Mănescu, V., et al. (2022). Magnesium-based alloys used in orthopedic surgery. Materials, 15(3), 1148.